

# Multi-reference-depth site response at the Garner Valley Downhole Array

J.P. Vantassel & B.R. Cox

*University of Texas at Austin, Austin, Texas, USA*

**ABSTRACT:** This paper compares empirical and theoretical site response using several different reference depths/conditions at the Garner Valley Downhole Array (GVDA). Empirical transfer functions (ETFs) from small amplitude ground motions are compared with 1D linear-viscoelastic theoretical transfer functions (TTFs) calculated using shear wave velocity ( $V_s$ ) profiles obtained from both invasive and non-invasive seismic testing. A previous study at the GVDA demonstrated that suites of non-invasive  $V_s$  profiles produced TTFs that better matched ETFs between bedrock and the surface than TTFs developed from invasive  $V_s$  profiles. However, comparisons for other reference depths/conditions were not considered. This study shows that suites of non-invasive  $V_s$  profiles at the GVDA also produce more accurate TTFs than those from invasive  $V_s$  profiles for all reference depths/conditions, and that estimates of the fundamental site frequency from horizontal-to-vertical spectral ratios can be used as an effective metric to determine an appropriate reference condition in forward site response analysis.

## 1 INTRODUCTION

This study compares measured and predicted linear-viscoelastic site response at a downhole array site in Southern California, called the Garner Valley Downhole Array. Generally speaking, downhole arrays consist of at least two accelerometers; one located at the ground surface and one at some depth below the ground surface. Placing sensors at varying depths allows for multiple recordings of seismic ground motions, providing insight into the frequency dependent amplification of waves as they propagate upward to the ground surface. Ideally, at least one of the subsurface accelerometers is placed within a competent reference material (i.e. rock-like conditions) to capture ground motions unmodified by the overlying soil layers. A major benefit of using downhole array recordings is that the site's measured response can be compared against numerical predictions without the uncertainty involved in estimating input ground motions at the subsurface reference condition. Frequency-dependent site amplification is often quantified in terms of a transfer function. A transfer function is the ratio of the Fourier amplitude spectra of two recorded acceleration time histories made at different depths during the same seismic event. The benefit of using transfer functions over, say, amplification factors from response spectral ratios is that the frequency domain representation of an acceleration time history is unique, meaning no information is lost in the transformation, whereas this is not true for a response spectra. Therefore, transfer functions provide a way of examining the fundamental component of site response without masking its insights through non-unique transformations. Transfer functions between the ground surface and underlying bedrock are most often sought in order to infer rock-to-soil amplification, but it is possible to obtain transfer functions between the ground surface and any underlying reference

depth/condition. This study will focus on comparing empirical and theoretical multi-reference-depth transfer functions as a means for evaluating the reliability of invasive and non-invasive shear wave velocity profiles and the appropriate reference condition needed to capture the site's global response.

## 2 THE GVDA SITE

The Garner Valley site was first instrumented with seismic monitoring equipment in 1989. Over time, it has come to consist of an instrumented downhole array, a liquefaction array, a simplified structure with foundation, and a rock reference site. This study will focus solely on the instrumented downhole array, which is known as the Garner Valley Downhole Array (GVDA). The GVDA consists of three surface accelerometers and six accelerometers located at various depths below the surface. The deepest sensor, located at 500 m, was not utilized in this study as the horizontal component recordings are unavailable. Furthermore, Teague et al. (2018) has shown that the three surface accelerometers provide similar results and therefore, as a simplification, only the northern-most surface accelerometer (00), which resides closest to the downhole accelerometers, has been used in this study. Thus, the six accelerometers used in this study are indicated in Figure 1 and numbered sequentially, with accelerometer 00 at the ground surface and 05 at a depth of 150 m. The site geology, also shown in Figure 1, is comprised of 18 – 25 m of mostly sandy- to silty-sand alluvium (AL), overlying decomposed granite (DG) to a depth of approximately 88 m, where competent, unweathered granite (GRNT) is located. However, the degree of weathering and depth to GRNT are believed to vary across the site.

The GVDA has been well-characterized by a number of invasive and non-invasive geotechnical and geophysical testing programs. This study will focus on three testing programs aimed at characterizing the site's small-strain shear stiffness through the measurement of shear wave velocity ( $V_s$ ) with depth. The considered testing programs are divided into two categories: invasive and non-invasive. In the invasive category is downhole testing (DH) performed by Gibbs (1989) and P- and S- suspension logging (PS) performed by Stellar (1996). In the non-invasive category is active-source and passive-wavefield surface wave testing performed by Teague et al. (2018) utilizing the layering ratio ( $\Xi$ ) inversion method proposed by Cox and Teague (2016) to account for  $V_s$  uncertainty. Figure 1 shows a comparison between  $V_s$  profiles from the DH, PS, and six surface wave  $\Xi$  inversions. Note that the PS profile is a "smoothed" or simplified profile developed by Teague et al. (2018). The dashed lines in Figure 1 show where the PS and DH profiles have been extended beyond their maximum depth of investigation to allow for their use with sensor 05 in a manner consistent with Teague et al. (2018). For each of the six surface wave  $\Xi$  inversions a suite of 99 non-unique but equally acceptable  $V_s$  profiles are shown (transparent lines) along with a representative median profile (opaque lines). While visually different, these 600  $V_s$  profiles developed from surface wave inversions all fit the experimental site signature, which consists of: (1) broadband surface wave dispersion data, and (2) an estimate of the fundamental site frequency ( $f_{0\_site}$ ) obtained from horizontal-to-vertical (H/V) spectral ratio noise data (i.e.  $f_{0\_H/V}$ ). From an examination of Figure 1, it is clear that the invasive and non-invasive profiles show reasonable agreement in the upper 50 m, however, below this depth the invasive and non-invasive profiles diverge. The non-invasive profiles generally indicate higher  $V_s$  at shallower depths than the invasive profiles. However, the invasive DH and PS profiles also vary significantly from one another in terms of the depth to competent rock ( $\sim 20$  m), as indicated by  $V_s$  greater than 1000 m/s. The effects of these different  $V_s$  profiles on the predicted linear-viscoelastic site response are investigated herein through comparison of empirical transfer functions (ETF) calculated from the recorded ground motion data and theoretical transfer functions (TTF) calculated from the measured  $V_s$  profiles.

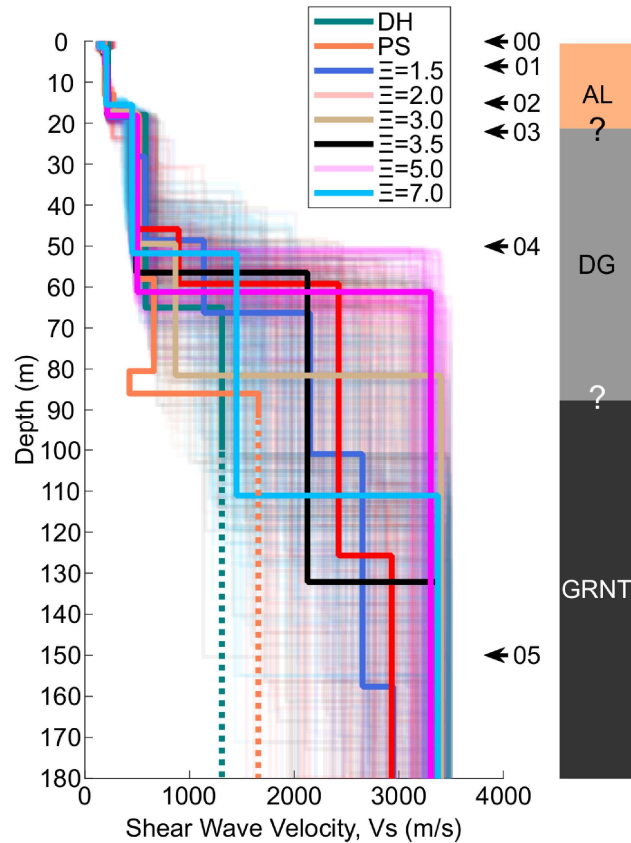


Figure 1. Invasive and non-invasive shear wave velocity ( $V_s$ ) profiles for the Garner Valley Downhole Array (GVDA) with the locations of six downhole array sensors (00–05) indicated alongside a schematic representation of the site’s geology illustrating the approximate thicknesses of alluvium (AL) and decomposed granite (DG) which overlay competent granite (GRNT). Invasive  $V_s$  profiles include those measured using downhole (DH) and P- and S- suspension logging (PS). Invasive  $V_s$  profiles have been extrapolated below their maximum investigation depths (shown with dotted lines) to reach the deepest reference sensor (05) and in a manner consistent with previous work at the GVDA. Non-invasive profiles include six suites of 99  $V_s$  profiles (transparent) derived from layering ratio ( $\Xi$ ) inversions of surface wave data. The six suites of 99 non-invasive  $V_s$  profiles are each represented by their layer-by-layer median  $V_s$  profile (opaque).

### 3 GROUND MOTION PROCESSING

Ground motions from the six GVDA accelerometers were downloaded from the NEES@UCSB data portal ([nees.ucsb.edu/data-portal](http://nees.ucsb.edu/data-portal)). The initial suite of candidate motions were the 50 selected by Tao & Rathje (2017) and subsequently used by Teague et al. (2018) for comparing site response between the competent bedrock accelerometer and the ground surface. These 50 motions had peak ground acceleration (PGA) values between 0.001 and 0.01 g, indicating that they propagated through the site in the small-strain, linear-viscoelastic range. All ground motion records were processed using a method adapted from Tao & Rathje (2017, 2019) to determine a single common bandwidth over which an acceptable signal-to-noise ratio (SNR) existed for all horizontal components of all sensors. To maintain a suitable frequency bandwidth with a SNR > 3dB across all sensors, it was not possible to utilize all 50 motions previously used. Ultimately, only 20 of the initial 50 candidate ground motions were selected for use in this study. These 20 motions had acceptable SNRs on all horizontal components of all sensors between 0.9 and 30 Hz. Importantly, this bandwidth encompassed the  $f_{0\_site}$  at GVDA, which is known to be  $\sim 2$ Hz from numerous H/V noise measurements (Teague et al. 2018).

## 4 RESULTS

### 4.1 Empirical Transfer Functions

After the final suite of 20 ground motions were appropriately processed and transformed into the frequency domain, ETFs were calculated between all 15 possible sensor pair combinations. For the sake of brevity, and to illustrate the most interesting points, this paper will focus only on the transfer functions between the sensor at the ground surface (00) and the five sensors located at depth (01 – 05). The calculation of the ETF involves simply dividing the frequency domain representation of the ground motion at the location of interest, in this case the surface, by the frequency domain representation of the ground motion recorded at the desired reference location. Figure 2 shows, for each surface/depth pair: the 20 ETFs (thin solid black lines), their lognormal median (thick solid colored line), and  $\pm$  one lognormal standard deviation (thick dashed colored line) for both the NS and EW components. A qualitative assessment of the ETFs reveals little variation between the horizontal components and particularly good agreement between both the location and amplitude of the response peaks for any given pair of sensors. The reader will note that while each peak in the ETF represents resonant frequencies of the soil column, these resonant frequencies are only descriptive of that portion of the soil column between the two sensors and are not necessarily representative of the site’s global behavior experienced by an earthquake event.

### 4.2 Comparison of Empirical and Theoretical Transfer Functions

Theoretical transfer functions (TTF) were developed using the invasive and non-invasive  $V_s$  profiles. The TTF is a numerical solution of the 1D wave equation for linear-viscoelastic layered media over linear-viscoelastic bedrock (Krammer 1996). All TTFs presented herein were calculated for “within” conditions so the results would be comparable to the ETFs, which were calculated relative to ground motions recorded within the soil column. The solution to the 1D wave equation in the linear-viscoelastic range requires the definition of the  $V_s$ , mass density, and small-strain damping ratio. The  $V_s$  profiles used are shown in Figure 1. The mass density was correlated from  $V_s$  using relationships by Mayne (2001). The small-strain damping ratio was obtained from the relationships by Darendeli (2001). Comparisons between the ETFs and TTFs are shown in Figure 3. The invasive  $V_s$  profiles are represented in Figure 3 by the TTFs calculated from the DH and smoothed PS results. The non-invasive  $V_s$  profiles are represented in Figure 3 by a single Median  $\Xi$  transfer function, (i.e. the lognormal median of the transfer functions derived from all six sets of 99  $V_s$  profiles presented in Figure 1). The Median  $\Xi$  TTF was calculated in this way to be consistent with previous work at the GVDA by Teague et al. (2018). It is noted that the TTF amplitudes from the DH and PS profiles are not directly comparable to the Median  $\Xi$  TTF amplitude, as the prior are singular observations and the later the median of observations that account for both epistemic uncertainty and aleatory variability. Thus, the TTF amplitudes from the DH and PS profiles are expected to be higher. Teague et al. (2018) attempted to lower the amplitudes of the DH and PS TTFs by performing  $V_s$  randomization to account for aleatory variability. However, this resulted in DH and PS TTF amplitudes that were much too low. Thus, in the present paper, we have chosen to make relative TTF comparisons as shown in Figure 3.

Two important elements should be discussed with respect to Figure 3; namely, the ability of TTFs from invasive and non-invasive  $V_s$  profiles to predict the ETF in terms of: (1) resonant frequencies, and (2) their corresponding amplitudes. First, TTFs from invasive and non-invasive  $V_s$  profiles show relatively good agreement with one another in terms of the first two, and in certain cases three, resonant frequencies of the truncated soil column. The only exceptions occur at the shallowest (i.e. 00/01) and deepest (i.e. 00/05) reference locations, where differences in the TTF fundamental resonant frequencies ( $f_{0\_TTF}$ ) derived from the invasive DH and PS  $V_s$  profiles are evident relative to the ETF fundamental resonant frequencies ( $f_{0\_ETF}$ ). Outside of these two reference depths, the invasive and non-invasive methods are shown to exhibit equal ability to capture the fundamental and first-higher modes evident in the ETFs, and in certain cases (i.e. 00/03 and 00/04) up to the second-higher mode. Indicating, that both the invasive and non-invasive  $V_s$  profiles appear to be capturing the site stiffness quite well across most depths. The lack of a clear

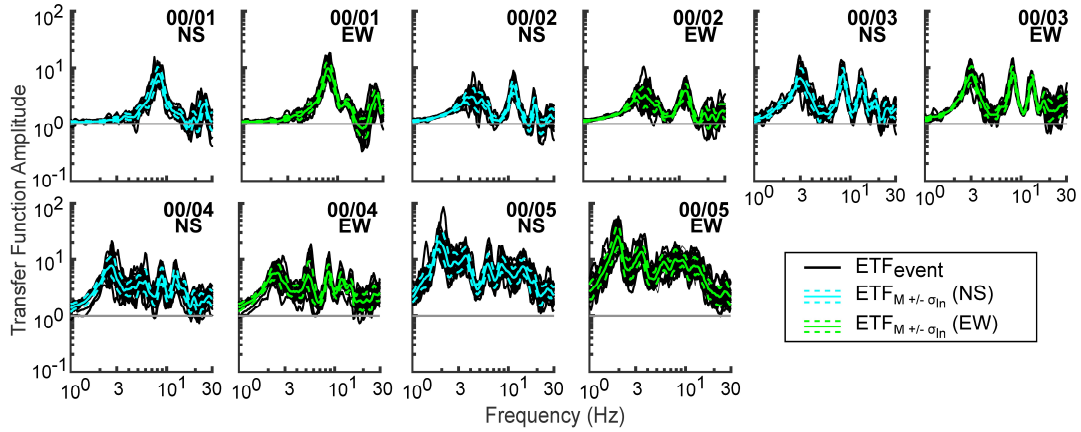


Figure 2. Empirical transfer functions (ETFs) for the final suite of 20 ground motions for the North-South (NS) and East-West (EW) components calculated between the seismometer at the ground surface (00) and those at five different reference depths (01, 02, 03, 04, and 05). The ETFs for each event (thin solid black line) are shown for each accelerometer pair with the lognormal median and  $\pm$  one lognormal standard deviation (solid and dashed thick colored lines) ETF used to statistically represent all events.

fundamental mode peak in the 00/02 ETFs is, in the opinion of the authors, evidence of an issue with the 02 sensor's ability to accurately capture low frequencies, as the higher modes of vibration show favorable comparisons with those predicted from the TTFs. For those two reference depths where the TTFs from invasive and non-invasive profiles do not agree favorably (i.e. 00/01 and 00/05), the TTFs from non-invasive profiles are shown to better capture the  $f_{0\_ETF}$  than those from the invasive profiles. With the invasive profiles appearing to be slightly off in terms of accurately representing the site's stiffness near the ground surface (i.e. 00/01) and the hard rock transition (i.e. 00/05). This demonstrates that suites of non-invasive profiles can equally, if not better, capture the site's resonant frequencies at all reference depths, provided those Vs profiles fit the experimental site signature.

Second, TTFs from invasive and non-invasive profiles are shown to have significantly different amplification at their resonant frequencies. The TTFs from non-invasive surface wave Vs profiles are shown to be consistently lower than those from the invasive DH and PS profiles. This amplitude difference is due to the averaging of many individual TTFs implicit in obtaining the Median  $\Xi$  TTF from the surface wave Vs profiles. Yet, despite the Median  $\Xi$  TTF from non-invasive profiles being much lower than the individual TTFs from the invasive DH and PS profiles, all TTFs still consistently overestimate the ETF's resonant amplification. Note that the one exception for this overestimation is the 00/05 sensor pair, where the amplitude of the Median  $\Xi$  TTF matches the ETF amplitude very well, as noted by Teague et al. (2018). Since the amplitude of the Median  $\Xi$  TTF between 00/05 matched quite well, we expected that the amplitudes of the Median  $\Xi$  TTFs and ETFs for the other reference depths would also agree well, however, this was not observed. Apparently, the near-surface variability (i.e. at depths between sensor 04 and the surface) present at the GVDA site is more significant than what the surface wave Vs profiles in Figure 1 indicate. The general inability to accurately model small-strain site response recorded at borehole array sites is well understood. As such, a number of researchers (e.g. Afshari & Stewart 2015, Tao & Rathje 2019) have sought for proxies/model adjustments that can be used to account for subsurface variability in 1D site response. These proxies include modifications to the small-strain soil damping ratio and Vs profile randomization. While these modifications can be successful at enabling a better match to the site response recorded at some borehole array sites, it is currently impossible to know a-priori which sites require modification, and to what extent. This is an area which will certainly require further study. Nonetheless, the non-unique Vs profiles derived from surface wave inversion did allow the site resonant frequencies to be preserved while lowering the Median  $\Xi$  TTF amplitudes at all reference depths, and generated a very accurate estimate of the amplitude of the most important transfer function between bedrock and the ground surface.

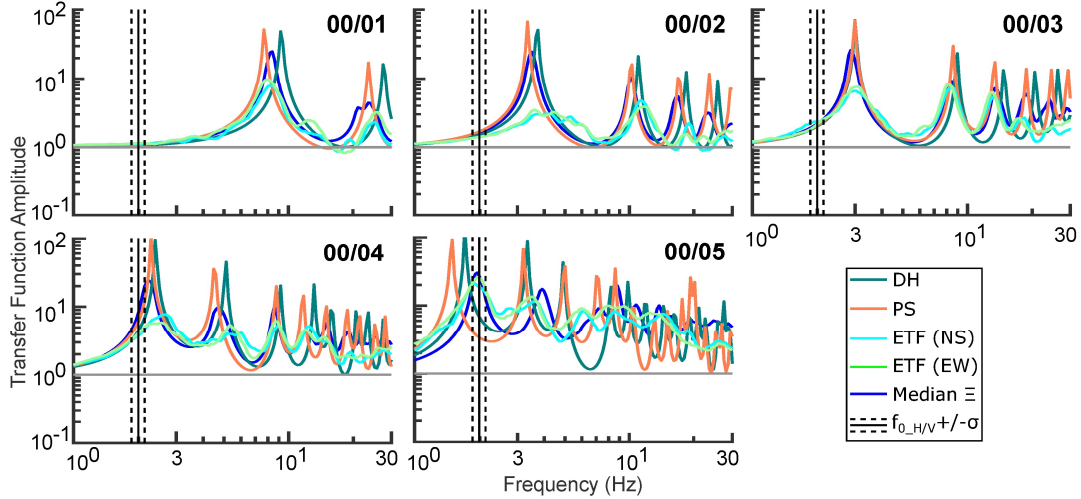


Figure 3. Comparison of empirical and theoretical transfer functions from invasive and non-invasive shear wave velocity ( $V_s$ ) profiles. For the five surface/depth accelerometer pairs the empirical transfer functions (ETFs) are compared to the theoretical transfer functions (TTFs) from the invasive and non-invasive  $V_s$  profiles shown previously in Figure 1. The non-invasive profiles are represented by the TTFs from the downhole (DH) and smoothed P- and S- suspension log (PS) profiles respectively. The non-invasive profiles are represented by the median layering ratio (Median  $\Xi$ ) TTF, which is the lognormal median of the transfer functions derived from all six sets of 99  $V_s$  profiles presented in Figure 1. The transfer functions are shown in reference to the mean and  $\pm$  one sigma fundamental site frequency ( $f_{0\_site}$ ) estimates obtained from horizontal-to-vertical spectral ratio (HVSr) noise measurements ( $f_{0\_H/V}$ ) made at the site.

In addition to examining our ability to predict multi-reference-depth site response, Figure 3 can help us to understand what constitutes a sufficient reference condition to capture the site's global behavior, specifically the  $f_{0\_site}$ . To illustrate this, the ETFs and TTFs are shown in comparison to the  $f_{0\_site}$  inferred from  $f_{0\_H/V}$  values presented by Teague et al. (2018), specifically  $f_{0\_H/V} \pm \sigma = 2.00 \pm 0.14$  Hz. Note that  $f_{0\_H/V}$  is shown to be a good estimate of  $f_{0\_site}$ , as indicated by the good agreement with  $f_{0\_ETF}$  for the deepest reference condition (i.e. 00/05 in Figure 3). Figure 3 shows that for each of the sensor pairs, with the exception of 00/05, the  $f_{0\_ETF}$  and  $f_{0\_TTF}$  overestimate the  $f_{0\_site}$  inferred from the  $f_{0\_H/V}$ . The  $f_{0\_site}$  is best understood to be related through the quarter wavelength approximation as the ratio between the height and stiffness of the soil column, where high frequencies indicate shallow and/or stiff conditions and low frequencies indicate deep and/or soft conditions (Vantassel et al. 2018). The  $f_{0\_ETF}$  and  $f_{0\_TTF}$  for all sensor pairs but 00/05 are overestimated relative to the  $f_{0\_H/V}$ , indicating that the corresponding site conditions and reference depths are either too stiff or too shallow, respectively, to accurately capture the site's global resonance. On the other hand, the  $f_{0\_ETF}$  and the non-invasive Median  $\Xi$   $f_{0\_TTF}$  for the 00/05 pair show good agreement with the  $f_{0\_H/V}$ , indicating an appropriate site reference condition has been achieved. However, for the 00/05 pair the  $f_{0\_TTF}$  obtained from the extrapolated DH and PS profiles underestimate the  $f_{0\_H/V}$ . This would indicate that the site conditions inferred by these profiles are too soft to accurately capture the site's global response. This discrepancy will be examined in detail in the following section.

#### 4.3 Discrepancy between Invasive and Non-Invasive TTFs at Depth

The underestimation of the  $f_{0\_site}$  by the DH and PS profiles at the deepest accelerometer was systematically investigated to determine at what depth or minimum velocity the GVDA site should be modeled in order to capture its global fundamental mode response. The investigation consisted of calculating TTFs for truncated  $V_s$  profiles between the surface and various depths (50 m to 175 m) and for the first exceedance of a common reference velocity representative of weathered rock (e.g. 760 m/s). These TTFs are shown in comparison to the aforementioned  $f_{0\_H/V}$  in Figure 4, which has been demonstrated to be a good estimate of the  $f_{0\_site}$ . The plots in Figure 4 illustrate a progression of the  $f_{0\_TTF}$  toward lower values as the depth of the truncated soil column

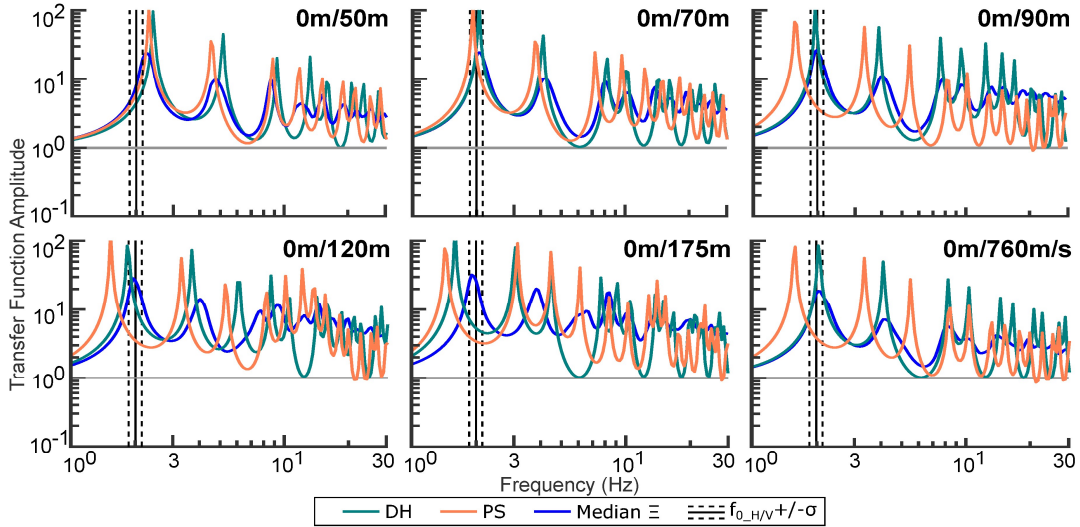


Figure 4. Comparison of theoretical transfer functions (TTFs) calculated from shear wave velocity ( $V_s$ ) profiles truncated at various depths between 50 and 175 m below the ground surface and at the first exceedance of a reference velocity of 760 m/s. The TTFs are shown in comparison to an estimate of the site's fundamental resonant frequency from horizontal-to-vertical spectral ratio (HVSr) noise measurements ( $f_{0\_H/V}$ ) made at the site.

is increased. When the  $V_s$  profiles are truncated at 50 m the invasive and non-invasive profiles both over-estimate the  $f_{0\_site}$ , clearly indicating the appropriate reference condition has not been reached. However, when the  $V_s$  profiles are truncated at 70 m both invasive and non-invasive profiles yield  $f_{0\_TTF}$  values that agree favorably with the  $f_{0\_site}$ . Interestingly, while a depth of 70 m below the ground surface is approximately 5 m below the last strong impedance contrast of the DH profile, no such impedance contrast is apparent in the PS profile at this depth, yet both yield good estimates of the  $f_{0\_site}$  (i.e. within one standard deviation of the  $f_{0\_H/V}$ ). This indicates that the selection of a reference condition based solely on the presence of a strong velocity contrast may not be sufficient to guarantee capture of the  $f_{0\_site}$ . With this in mind, the  $V_s$  profiles were truncated at 90 m, just below the last strong impedance contrast evident in the PS log. Even though this would appear to be a logical reference condition for the PS log, the PS  $f_{0\_TTF}$  clearly underestimates the  $f_{0\_site}$  and continues to shift to the left as the PS velocity profile is truncated at greater depths. The DH shows similar behavior starting at the 120 m reference depth, keeping in mind that the DH and PS profiles were extrapolated at a constant velocity below 100 m and 92 m respectively. From the quarter wavelength approximation we can understand this underestimation of the  $f_{0\_site}$  by the PS and DH profiles as the depth-to-stiffness ratio becoming too large (i.e. profiles are too soft to accurately predict the  $f_{0\_site}$ ). The non-invasive profiles, however, are able to accurately capture the  $f_{0\_site}$  at each depth below 70 m. This indicates that the non-invasive  $V_s$  profiles are accurately capturing the site's increase of stiffness with depth such that the  $f_{0\_site}$  is preserved regardless of the reference depth chosen. The  $V_s$  profiles were also truncated at the first exceedance of  $V_s = 760$  m/s, which is a commonly assumed reference condition for soft/weathered rock. In this case, the DH and Median  $\Xi$  TTFs provide good estimates of the  $f_{0\_site}$ , while the PS TTF significantly underestimates the  $f_{0\_site}$ . Once again, this illustrates that blind application of a given velocity reference condition may not yield accurate predictions of frequency dependent site amplification.

## 5 CONCLUSION

This study has shown that non-unique  $V_s$  profiles derived from surface wave measurements at the GVDA are able to accurately predict multi-reference-depth site response in terms of  $f_{0\_TTF}$  that are very similar to  $f_{0\_ETF}$ , despite visually-significant differences in the inverted  $V_s$  profiles. The invasive  $V_s$  profiles from DH and PS measurements were also able to yield  $f_{0\_TTF}$  that were similar

to  $f_{0\_ETF}$  calculated between the ground surface and most subsurface sensor locations. However, they could not accurately predict  $f_{0\_ETF}$  measured between the surface and the shallowest and deepest sensors (i.e. 01 and 05, respectively). Furthermore, the amplitudes of the TTFs obtained from the DH and PS profiles were significantly greater than those obtained from the median ETFs at all depths. While the Median  $\Xi$  TTFs obtained from the non-invasive surface wave Vs profiles had amplitudes that were closer to those of the median ETFs at all reference depths, they still overestimated amplitudes for all reference conditions with the exception of the deepest sensor (i.e. 05). This finding was unanticipated, as we expected the non-unique Vs profiles obtained from surface wave inversion to better match the EFT amplitudes at all reference depths. Clearly more work is needed to more accurately predict small-strain, linear-viscoelastic site response amplitudes. This study has also shown that the blind use of Vs profiles truncated at a strong velocity contrast or a specific velocity condition may not guarantee accurate representation of the site's global response. Thus, it is recommended that estimates of  $f_{0\_site}$  be made via H/V spectral ratio noise measurements, and that this value (i.e.  $f_{0\_H/V}$ ) be used to screen Vs profiles to determine an appropriate reference depth that is consistent with the  $f_{0\_site}$ .

## 6 ACKNOWLEDGEMENTS

This work was supported primarily by U.S. National Science Foundation (NSF) grant CMMI-1261775. However, any opinions, findings, and conclusions or recommendations expressed in this material are those of the authors and do not necessarily reflect the views of NSF.

## REFERENCES

- Afshari, K., & Stewart, J. P. 2015. Effectiveness of 1D ground response analyses at predicting site response at California vertical array sites. *Proc. SMIP15 Seminar on Utilization of Strong-Motion Data, California Strong Motion Instrumentation Program (CSMIP), Davis, 22 October 2015.*
- Cox, B. R. & Teague, D. P. 2016. Layering ratios: a systematic approach to the inversion of surface wave data in the absence of A-priori information. *Geophys J Int*, 207:422–38.
- Darendeli, M. B. 2001. Development of a new family of normalized modulus reduction and material damping curves (Ph.D. Dissertation). Austin, TX: The University of Texas.
- Gibbs, J. F. 1989. Near-surface P- and S-wave velocities from borehole measurements near Lake Hemet, California. U.S. Geological Survey Open File Report.
- Kramer, S. L. 1996. *Geotechnical Earthquake Engineering*. New Jersey: Prentice Hall.
- Mayne, P. 2001. Stress-strength-flow parameters from enhanced in-situ tests. *Proc. Intern. Conf. on In-Situ Measurement of Soil Properties & Case Histories [In-Situ 2001], Bali, Indonesia, 21-24 May 2001.*
- Steller, R. 1996. New borehole geophysical results at GVDA. UCSB Internal report.
- Tao, Y. & Rathje, E. M. 2017. Insights into Small-strain Damping from Downhole Array Recordings. *Proc. of the 2017 Annual Meeting of the Seismological Society of America, Denver, 18-20 April 2017.*
- Tao, Y. & Rathje, E. M. 2019. Insights into Modeling Small-Strain Site Response Derived from Downhole Array Data. *Journal of Geotechnical and Geoenvironmental Engineering*. (accepted).
- Teague, D. P., Cox, B. R., & Rathje, E. M. 2018. Measured vs. predicted site response at the Garner Valley Downhole Array considering shear wave velocity uncertainty from borehole and surface wave methods. *Soil Dyn and Earthq Eng*, 113:339-355.
- Vantassel, J., Cox, B., Wotherspoon, L., & Stolte, A. 2018. Mapping Depth to Bedrock, Shear Stiffness, and Fundamental Site Period at CentrePort, Wellington, Using Surface-Wave Methods: Implications for Local Seismic Site Amplification. *Bulletin of the Seismological Society of America* 108(3B): 1709–1721.